Asian Journal of Chemistry; Vol. 30, No. 7 (2018), 1645-1649

ASIAN JOURNAL OF CHEMISTRY

https://doi.org/10.14233/ajchem.2018.21298

Removal of Orange 2G Dye from Aqueous Solutions Using TiO_2-Based Nanoparticles: Isotherm and Kinetic Studies

A.A. AL-ARFAJ*, F. ALAKHRAS, E. AL-ABBAD, N.O. ALZAMEL, N.A. AL-OMAIR and N. OUERFELLI

Department of Chemistry, College of Science, Imam Abdulrahman Bin Faisal University, P.O. Box 1982, Dammam 31441, Saudi Arabia

*Corresponding author: E-mail: ahalarfaj@iau.edu.sa

Received: 21 February 2018; *Accepted*: 25 April 2018; *Published online*: 31 May 2018; AJC-18947

In the current study, the removal of Orange 2G dye founded in aqueous solutions using titanium dioxide-based nanoparticles has been investigated. Titanium dioxide nanoparticles were successfully prepared using tetrabutyl ammonium bromide (T_{TAB}) as a surfactant by sol-gel method and characterized by X-ray diffraction, BET surface area, IR and TEM spectroscopy. The experimental data is most fitting with Freundlich isotherm model indicating heterogeneity of sorbent surface. Langmuir data revealed that the maximum removal capacity of Orange 2G equals to 85.47 mg g^{-1}. Kinetic studies disclosed that intraparticle diffusion is not the only rate-determining step and the removal process is organized by a chemical reaction as well.

Keywords: TiO_2 nanoparticles, Orange 2G dye, Water treatment, Sorption, Langmuir isotherm, Kinetic studies.

INTRODUCTION

Hazardous wastes are toxic byproducts of oil, petrochemicals and other industrial. About 20 % of dyes produced globally are released to the environment as part the dyeing processes wastewater [1]. Azo dyes, which are identified when the azo bonds (N=N) are one compositions of the dyes are the most harmful pollutants associated with industries utilizing dyeing in their manufacturing processes such as the food industries, cosmetics, printing and pharmaceuticals. As a result, the wastewater generated from such industries is considered extremely toxic to humans and to the adjacent environments due to the dyes non-degradability, toxicity and carcinogenicity [2]. The development of innovative and cost effective processes for treating contaminated wastewater from toxic dyes is considered a challenge and critical at the same time for such industries. With the boom of nanotechnologies and its applications, it was intensively investigated to measure the application of nanotechnology to extract the toxic dyes from the contaminated wastewater [3,4]. The physical or chemical separation of pollutants from an aqueous solution is the key element in wastewater treatment since it simplify the purification processes and require a knowledge of the rate law describing the extraction kinetics. Separation by adsorption is considered an effective and cost efficient method for heavy metal treatment. The adsorption by cross-linked polymers possesses illustrated is very easy to manipulate by design and experimentally due to its ability for regeneration [5-12]. Adsorption is a solid method for the removal of low concentrations of organic compounds from large volumes of potable water, process effluents, wastewater and aqueous solutions. Adsorption by using activated carbon is an efficient and cost effective method for removing organic compounds in diluted aqueous solutions [13]. Titanium dioxide (TiO_2) is a stable and non-toxic compound [14] that has been proven highly effective in the removing of organic compounds due to its large surface area, uniform meso-porosity and its biocompatibility [15].

In continuation of our previous work [4], TiO_2 nanoparticles using tetrabutyl ammonium bromide (T_{TAB}) as a surfactant were synthesized by sol-gel method and used for removal of Orange 2G dye from wastewater under UV light. The effects of pH, concentration of pollutant, contact time and doses of TiO_2 were investigated. The acquired data revealed that the TiO_2 nanoparticles prepared with T_{TAB} had 98 % of percentage removal under optimal conditions of 4.0 g L^{-1} dosage, pH = 3, agitation period of 28 h with initial dye concentration of 1.5×10^{-5} mol L^{-1}.

In this paper we report on the data of Freundlich, Langmuir and Temkin isotherm models for investigating the equilibrium behaviour and evaluating the sorption capacity of the prepared nanoparticles toward Orange 2G removal. Additionally, to understand the effect of exposure time and the kinetics of removal process, more investigation should be done and presented in this article. Pseudo-first order and pseudo-second order kinetic models will be used for the analysis. Furthermore, the intraparticle diffusion model which is developed to inspect

the mechanism of discarding for a solid-liquid disposal process will be applied as well.

EXPERIMENTAL

All chemicals were used as received without further processing or enhancements. Titanium tetrachloride ($TiCl_4$. 99 %), ethanol, tetrabutyl ammonium bromide (T_{AB}) were purchased from Sigma- Aldrich Ltd. Azo dye Orange 2G, 4-[(2-hydrox-1-naphthayl-)azobenzene sulphonic acid monosodium salt, ($C_{16}H_{11}N_2O_4SNa$) was obtained from Aldrich.

Preparation and characterization of TiO_2 nanoparticles: TiO_2 nanoparticles were synthesized and intensively characterized depending on a process reported previously [4]. The nanoparticles were generated using tetrabutyl ammonium bromide (T_{TAB}) as a surfactant by sol-gel method. X-ray diffraction (XRD) was recorded, BET surface area and mean pore radius (r) was determined from N_2 adsorption isotherm. Surface morphology and microstructure was investigated by TEM whereas, UV-visible absorption was obtained with Perkin-Elmer Lambda 40 spectrophotometer.

Photocatalytic removal of Orange 2G dye by TiO_2 nanoparticles: The photocatalytic activity of synthesized TiO_2 nanoparticles was investigated for the removal of Orange 2G Dye. The experiments were explored by batch equilibrium method. Each trial consisted of mixing 100 mL of dye solution with initial concentration ranging from 5.25-35.03 mg L^{-1} at pH 3 with 0.05 g nanoparticle dosage. The mixture solution was shaken for a predefined time from 1 to 24 h. After the mixing time elapsed, the mixture was allowed to settle and the solution was analyzed for the residual dye by measuring the absorbance intensity at 485 nm. All experiments were performed at room temperature.

Data analysis: The experimental data were used to calculate Orange 2G Dye % removal in accordance with the following equation:

$$\text{Removal (\%)} = \frac{C_o - C_t}{C_o} \times 100 \quad (1)$$

where, C_o (mg L^{-1}) is the initial concentration and C_t (mg L^{-1}) is 2G Dye concentration at time t. The adsorption capacity, the amount of 2G Dye removed per mass-unit of the nanoparticle, was determined using the following equations:

The adsorption capacity at equilibrium, Q_e (mg g^{-1}):

$$Q_e = \frac{(C_o - C_e)V}{m} \quad (2)$$

The adsorption capacity at time t, Q_t (mg g^{-1}):

$$Q_t = \frac{(C_o - C_t)V}{m} \quad (3)$$

where, C_e (mg L^{-1}) is the equilibrium concentration of Orange 2G Dye, m (g) is the mass of nanoparticle and V (L) is the volume of dye solution. C_t (mg L^{-1}) is the residual dye concentration at different period t.

RESULTS AND DISCUSSION

Characterization of synthesized TiO_2 nanoparticles: TiO_2 Nanoparticles were successfully prepared using tetrabutyl ammonium bromide (T_{TAB}) as a surfactant by sol-gel method. The XRD data designated that the crystalline phase of nanoparticles is mainly anatase structure with crystal size of 17.7 nm. BET measurements revealed the surface area and mean pore radius of T_{TAB} is 83.49 m^2 g^{-1} and 7.6 nm, respectively with ink-bottles shape. The lower value of surface area for T_{TAB} can be related to the formation of agglomeration of the crystallites during preparation of TiO_2 using tetrabutylammonium bromide [16]. FTIR spectra of TiO_2 samples were performed to estimate the features of the chemical status of their surface. T_{TAB} nanoparticles were characterized by the presence of a broad band around 3378 cm^{-1} and by a weak signal at 1628 cm^{-1} corresponding to the OH stretching and bending mode, respectively. These referable to the surface hydroxyl groups associated with adsorbed water. This can be confirming the organic-free surface of the TiO_2 [17]. The results also showed that TiO_2 nanoparticles have irregular shapes, aggregated and formed large particle blocks. A detailed analysis of XRD, IR spectra, surface morphology and BET surface area of the synthesized nanoparticles has been reported in previous work [4].

Equilibrium and isotherm studies: As can be clearly seen in Table-1 and Fig. 1, the effect of initial dye concentration on photocatalytic removal was well studied in the range of 5.25-35.03 mg L^{-1}. The experiments were presented and well performed at pH = 3 and 24 h of agitation time along with the adsorbent dosage of 0.05 g. It has been found that when the initial concentration increased, the removal capacity (Q_e) also increased from 10.29 to 64.88 mg g^{-1}. The results also have showed that if the initial solute concentrations are increased, the total percent removal is decreased as well (Fig. 2). However, at higher concentration the available sites of degradation became fewer compared to the number of dye moles. Therefore, the percentage removal would be dependent upon the initial dye concentration.

The experimental data of photocatalytic removal of Orange 2G dye were investigated by a linear plot of Langmuir, Freundlich and Temkin isotherm models [18,19] as depicted in the following equations, respectively.

Langmuir isotherm:

$$\frac{C_e}{Q_e} = \frac{1}{Q_o K_L} + \frac{C_e}{Q_o} \quad (4)$$

TABLE-1
REMOVAL OF ORANGE 2G DYE BY TiO_2 NANOPARTICLES AT DIFFERENT CONCENTRATIONS

pH	W (g)	V (L)	C_o (mg L^{-1})	C_e (mg L^{-1})	Q_e (mg g^{-1})	Removal (%)
3	0.05	0.1	5.25	0.11	10.29	98.00
	0.05	0.1	7.00	0.17	13.66	97.56
	0.05	0.1	10.51	0.35	20.31	96.63
	0.05	0.1	17.52	0.88	33.29	95.00
	0.05	0.1	24.52	1.44	46.16	94.13
	0.05	0.1	35.03	2.59	64.88	92.60

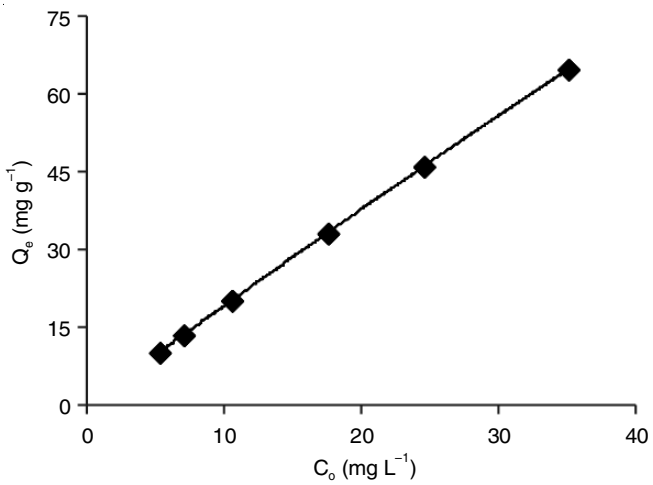

Fig. 1. Effect of Orange 2G dye solution concentration on the removal capacity of the synthesized TiO_2 nanoparticles

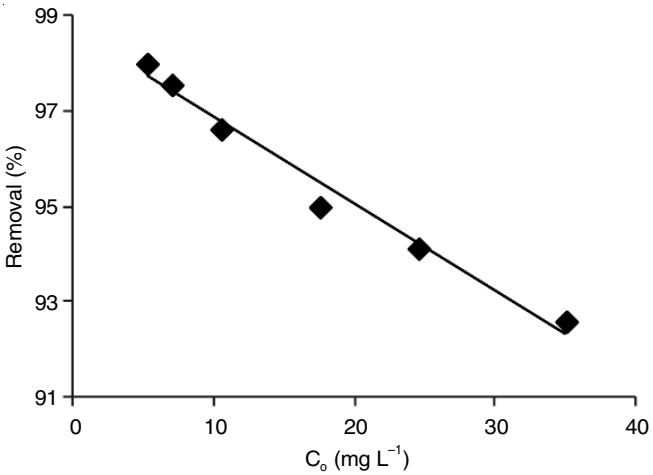

Fig. 2. Effect of Orange 2G dye solution concentration on the percentage removal of the synthesized TiO_2 nanoparticles

Freundlich isotherm:

$$\log Q_e = \log K_F + \frac{1}{n}\log C_e \quad (5)$$

Temkin isotherm:

$$Q_e = B\ln A + B\ln C_e \quad (6)$$

As can be seen in Table-2, the correlation coefficients pointed out that Freundlich isotherm is the most fitting and appropriate model to explain the removal of Orange 2G dye with $R^2 = 0.9994$. Nevertheless, the R^2 values for Langmuir and Temkin isotherms are still very close to that of Freundlich model. That means there are no certain and obvious pattern to explain the isotherm studies. Langmuir data disclosed that the maximum adsorption capacity (Q_o) equals 85.47 mg g^{-1}. The obtained value of adsorption coefficient (K_L) means that the energy of adsorption is convenient for Orange 2G dye with TiO_2 nanoparticles prepared using tetrabutyl ammonium bromide. Depending upon the impact of the separation factor, R_L, average is presented in Table-2, it was indicated that the values of R_L were between $0 < R_L < 1$, which gives a reasonable sign and proposition that the degradation of 2G dye by the sorbent is a favourable process [12].

K_F values which is indication of the adsorption capacity and 1/n demonstrating the favourability and encouragement of removal. Temkin isotherm model can also be used to explain the removal process. This model assumes that the adsorption energy decreased upon increasing in surface coverage with adsorbate species and the sorption process can be depicted by uniform distribution of biding energies up to maximum [20]. The heat of adsorption (constant B) is equal to 16.28 J mol^{-1} while the maximum binding energy (constant A) is equal to 13.15 L g^{-1}. Freundlich and Temkin models data confirm the favourability of degradation for 2G dye onto sorbent surface.

Kinetic studies: The kinetic parameters were carried out by using 35.03 mg L^{-1} of Orange 2G dye in pH 3 at room temperature. The remaining concentrations were examined during the interval time between 1 to 24 h. The collected data were fitted using three kinetic models: pseudo-first order, pseudo-second order and intraparticle diffusion model. The representative equations for the kinetic models are presented in Table-3, where Q_t and Q_e are the amount of Orange 2G dye removed at time t and at equilibrium in mg g^{-1}, respectively, k is the rate constant and C is the boundary thickness layer in mg g^{-1} [21,22]. Fig. 3 revealed that the percentage removal of Orange 2G dye is gradually increased by time and reached a steady state after 12 h of contact time. As can be clearly seen from Table-4, the values of Q_e that were calculated using pseudo-second order model were closer to the experimental one than using the first order model, assuming that chemisorption process has been taken out and the given data were suitably fitted with pseudo-second order kinetic model [23].

TABLE-3
LINEARIZED EQUATIONS FOR
ORANGE 2G DYE REMOVAL KINETICS

Kinetic model	Linear equation	Plot
Pseudo first-order	$\ln (Q_e - Q_t) = \ln Q_e - k_1 t$	$\ln (Q_e - Q_t)$ *vs.* t
Pseudo second-order	$\frac{t}{Q_t} = \frac{1}{k_2 Q_e^2} + \frac{t}{Q_e}$	$\frac{t}{Q_e}$ *vs.* t
Intraparticle diffusion	$Q_t = k_{id}\, t^{1/2} + C$	Q_t *vs.* $t^{1/2}$

The intraparticle diffusion model is developed to investigate the mechanism of sorption for a solid-liquid removal process. By applying the experimental data using intraparticle diffusion model, three zones can be appeared as shown in Fig. 4. The first zone was attributed to the diffusional process of the dye on the sorbent surface; hence, it was the fastest adsor-

TABLE-2
LANGMUIR, FREUNDLICH AND TEMKIN ISOTHERM MODELS PARAMETERS FOR THE REMOVAL OF ORANGE 2G DYE

Langmuir isotherm				Freundlich isotherm			Temkin isotherm		
Q_o (mg g^{-1})	K_L (L mg^{-1})	R_L	R^2	K_F (mg g^{-1}) (mg $L^{-1})^{1/n}$	n	R^2	B (J mol^{-1})	A (L g^{-1})	R^2
85.47	0.959	0.085	0.9395	37.09	1.75	0.9994	16.28	13.15	0.9333

TABLE-4
KINETIC CONSTANTS FOR PSEUDO FIRST-ORDER, PSEUDO SECOND-ORDER AND INTRAPARTICLE DIFFUSION MODELS FOR ORANGE 2G DYE SORPTION

$(Q_e)_{exp}$	Pseudo- first order			Pseudo-second order			Intraparticle diffusion model		
	$(Q_e)_{cal}$	K_1	R_1^2	$(Q_e)_{cal}$	K_2	R_2^2	k_{id}	C	R^2
64.88	34.71	1.8424×10^{-3}	0.7736	70.42	8.8463×10^{-5}	0.9924	1.9834	7.722	0.9968

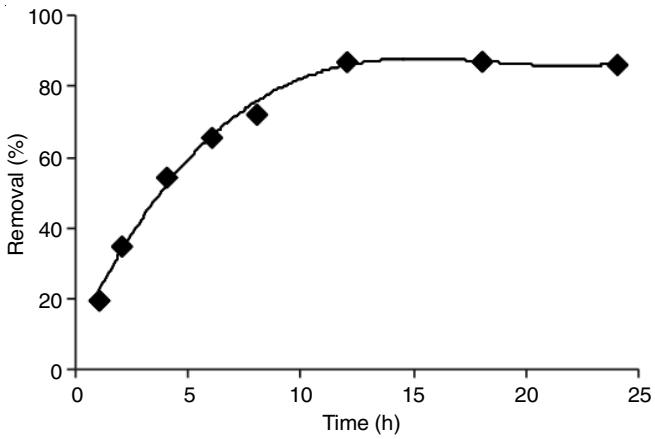

Fig. 3. Effect time on the percentage removal of the synthesized TiO_2 nanoparticles

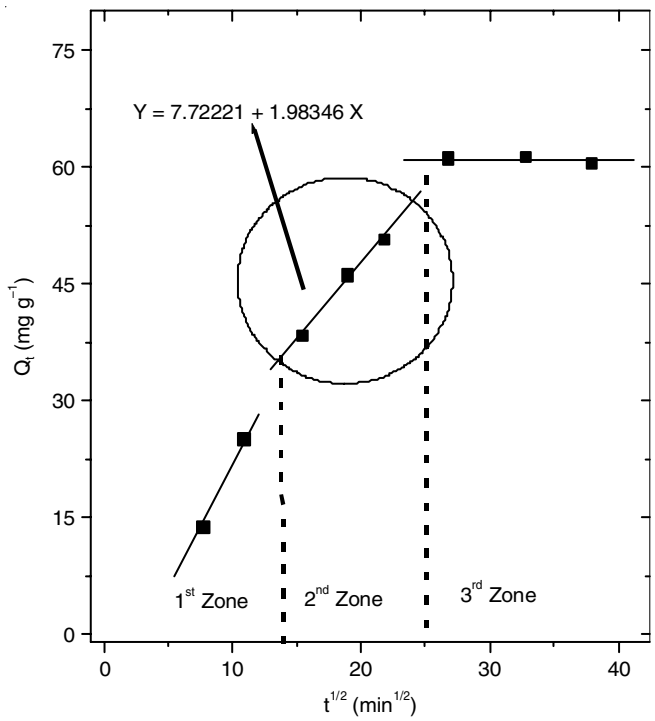

Fig. 4. Intraparticle diffusion plot for the removal of Orange 2G dye

ption period. The second section (2nd zone) was suggested to intraparticle diffusion, a delayed process. The third stage (3rd zone) could be regarded as the diffusion through smaller pores, which is followed by the establishment of equilibrium [24,25]. From the slope of the linear portion of the second zone it was possible to determine intraparticle diffusion rate constant (K_{id}) which is 1.9834 mg g^{-1} $min^{-½}$ and thickness boundary layer (C) which is 7.7222 mg g^{-1}. As shown in Fig. 4, the plot of the zone did not pass through the origin, indicating that intraparticle diffusion is not the only rate-determining step and the removal process is organized by a chemical reaction as well.

As appeared in Table-5, the comparative dye's uptake of different TiO_2-based nanoparticles shows that the investigated sorbent has better removal capacity than other TiO_2-based subsidiaries given in literature [26-30] showing high potential as a competent material for extraction of harmful species from polluted liquid sources.

Comparative removal of adsorption capacity of TiO_2 nanoparticles (T_{TAB}) with various reported adsorbents are given in Table-5.

Conclusion

The removal of Orange 2G dye from aqueous solutions using TiO_2 nanoparticles has been performed in the range of 5.25-35.03 mg L^{-1} at pH = 3 and 24 h of exposure time along with 0.05 g sorbent dosage. The quantity of residual dye has been estimated by measuring the absorbance intensity at 485 nm. It has been found that when the initial concentration increased, the removal capacity (Q_e) also increased from 10.29 to 64.88 mg g^{-1}. Freundlich isotherm model was represented the best elucidation for the experimental data; whereas the highest removal capacity (Q_0) equals 85.47 mg g^{-1}. The kinetics followed pseudo second-order model disclosed that the adsorption is chemisorption. Intraparticle diffusion data provided three linear plots indicating the sorption process is affected by two or more steps. The investigations may indicate that our target TiO_2-base nanoparticles are feasible as sorbent for the removal of toxic dyes from wastewater samples.

TABLE-5
COMPARATIVE REMOVAL OF ADSORPTION CAPACITY OF TiO_2 NANOPARTICLES (T_{TAB}) WITH VARIOUS REPORTED ADSORBENTS

Adsorbent	Removed dye	Adsorption capacity (mg g^{-1})	Ref.
Amylopectin-TiO_2-Au nanocomposite	Acidic orange (AO)	51.13	[26]
Mixed-phase P25 TiO_2 nanoparticles	Methyl orange (MO)	5.55	[27]
	Congo red (CR)	27.91	[27]
5-Sulfosalicylic acid grafted TiO_2 nanoparticles	Methylene blue (MB)	9.80	[28]
Chitosan-modified TiO_2 nanoparticles	Malachite green (MG)	6.30	[29]
Carbon-modified TiO_2 nanoparticles	Methyl orange (MO)	171.43	[30]
TiO_2 nanoparticles (T_{TAB})	Orange 2G	85.47	Present work

REFERENCES

1. M.C. Somasekhara Reddy, L. Sivaramakrishna and A.V. Reddy, *J. Hazard. Mater.*, **203-204**, 118 (2012); https://doi.org/10.1016/j.jhazmat.2011.11.083.
2. J. Sun, L. Qiao, S. Sun and G. Wang, *J. Hazard. Mater.*, **155**, 312 (2008); https://doi.org/10.1016/j.jhazmat.2007.11.062.
3. M. Pelaez, A.A. de la Cruz, E. Stathatos, P. Falaras and D.D. Dionysiou, *Catal. Today*, **144**, 19 (2009); https://doi.org/10.1016/j.cattod.2008.12.022.
4. S.M. Reda and A.A. Al-Arfaj, *J. Curr. Phys. Chem.*, **3**, 366 (2013); https://doi.org/10.2174/1877946811303030011.
5. A. Jakubiak, I.A. Owsik and B.N. Kolarz, *React. Funct. Polym.*, **65**, 161 (2005); https://doi.org/10.1016/j.reactfunctpolym.2004.10.006.
6. B.N. Kolarz, A. Jakubiak, J. Jezierska and B. Dach, *React. Funct. Polym.*, **68**, 1207 (2008); https://doi.org/10.1016/j.reactfunctpolym.2008.04.005.
7. M.R. Maurya, S. Sikarwar, T. Joseph, P. Manikandan and S.B. Halligudi, *React. Funct. Polym.*, **63**, 71 (2005); https://doi.org/10.1016/j.reactfunctpolym.2005.02.008.
8. K.C. Gupta and A.K. Sutar, *Polym. Adv. Technol.*, **19**, 186 (2008); https://doi.org/10.1002/pat.994.
9. K.C. Gupta and A.K. Sutar, *React. Funct. Polym.*, **68**, 12 (2008); https://doi.org/10.1016/j.reactfunctpolym.2007.10.015.
10. M. Ruiz, A.M. Sastre and E. Guibal, *React. Funct. Polym.*, **45**, 155 (2000); https://doi.org/10.1016/S1381-5148(00)00019-5.
11. F. Fu and Q. Wang, *J. Environ. Manage.*, **92**, 407 (2011); https://doi.org/10.1016/j.jenvman.2010.11.011.
12. O.C.S. Al Hamouz, *Arab. J. Sci. Eng.*, **41**, 119 (2016); https://doi.org/10.1007/s13369-015-1622-0.
13. O. Hamdaoui and E. Naffrechoux, *J. Hazard. Mater.*, **147**, 381 (2007); https://doi.org/10.1016/j.jhazmat.2007.01.021.
14. R.C. Bansal and M. Goyal, Activated Carbon Adsorption, Boca Raton, CRC Press, Taylor Francis Group (2005). https://www.taylorfrancis.com/books/9781420028812.
15. K. Bhattacharyya, *Appl. Clay Sci.*, **41**, 1 (2008); https://doi.org/10.1016/j.clay.2007.09.005.
16. V. Belessi, G. Romanos, N. Boukos, D. Lambropoulou and C. Trapalis, *J. Hazard. Mater.*, **170**, 836 (2009); https://doi.org/10.1016/j.jhazmat.2009.05.045.
17. G. Mascolo, R. Comparelli, M.L. Curri, G. Lovecchio, A. Lopez and A. Agostiano, *J. Hazard. Mater.*, **142**, 130 (2007); https://doi.org/10.1016/j.jhazmat.2006.07.068.
18. M.B. Ibrahim and S. Sani, *Open J. Phys. Chem.*, **4**, 139 (2014); https://doi.org/10.4236/ojpc.2014.44017.
19. W.S.W. Ngah and S. Fatinathan, *J. Environ. Sci. (China)*, **22**, 338 (2010); https://doi.org/10.1016/S1001-0742(09)60113-3.
20. A.O. Dada, A.P. Olalekan, A.M. Olatunya and O. Dada, *IOSR J. Appl. Chem.*, **3**, 38 (2012); https://doi.org/10.9790/5736-0313845.
21. H. Zhang, R.G. McDowell, L.R. Martin and Y. Qiang, *Appl. Mater. Interfaces*, **8**, 9523 (2016); https://doi.org/10.1021/acsami.6b01550.
22. A. Maleki, E. Pajootan and B. Hayati, *Taiwan Inst. Chem. Eng.*, **51**, 127 (2015); https://doi.org/10.1016/j.jtice.2015.01.004.
23. C. Noureddine, A. Lekhmici and M.S. Mubarak, *J. Appl. Polym. Sci.*, **107**, 1316 (2008); https://doi.org/10.1002/app.26627.
24. R.R. Sheha and A.A. El-Zahhar, *J. Hazard. Mater.*, **150**, 795 (2008); https://doi.org/10.1016/j.jhazmat.2007.05.042.
25. E.C. Lima, M.A. Adebayo and F.M. Machado, in eds.: C.P. Bergmann and F.M. Machado, Kinetic and Equilibrium Models of Adsorption in Carbon Nanomaterials as Adsorbents for Environmental and Biological Applications, Springer, pp. 33-69 (2015);
26. A.K. Sarkar, A. Saha, A. Tarafder, A.B. Panda and S. Pal, *ACS Sustain. Chem. Eng.*, **4**, 1679 (2016); https://doi.org/10.1021/acssuschemeng.5b01614.
27. D. Ljubas, G. Smoljanic and H. Juretic, *J. Environ. Manage.*, **161**, 83 (2015); https://doi.org/10.1016/j.jenvman.2015.06.042.
28. A. Mohammadi and A.A. Karimi, *J. Water Environ. Nanotechnol.*, **2**, 118 (2017); https://doi.org/10.22090/jwent.2017.02.007.
29. Z.M. Abou-Gamra and M.A. Ahmed, *Adv. Chem. Eng. Sci.*, **5**, 373 (2015); https://doi.org/10.4236/aces.2015.53039.
30. S. Jafari, Ph.D. Thesis, Investigation of Adsorption of Dyes onto Modified Titanium Dioxide, Acta Universitatis Lappeenrantaensis, Yliopistopaino, Finland (2016); http://urn.fi/URN:ISBN:978-952-265-970-5.